



Plasma Emission Characteristics From a High Current Hollow Cathode in an Ion Thruster Discharge Chamber

John E. Foster and Michael J. Patterson
Glenn Research Center, Cleveland, Ohio

The NASA STI Program Office . . . in Profile

Since its founding, NASA has been dedicated to the advancement of aeronautics and space science. The NASA Scientific and Technical Information (STI) Program Office plays a key part in helping NASA maintain this important role.

The NASA STI Program Office is operated by Langley Research Center, the Lead Center for NASA's scientific and technical information. The NASA STI Program Office provides access to the NASA STI Database, the largest collection of aeronautical and space science STI in the world. The Program Office is also NASA's institutional mechanism for disseminating the results of its research and development activities. These results are published by NASA in the NASA STI Report Series, which includes the following report types:

- **TECHNICAL PUBLICATION.** Reports of completed research or a major significant phase of research that present the results of NASA programs and include extensive data or theoretical analysis. Includes compilations of significant scientific and technical data and information deemed to be of continuing reference value. NASA's counterpart of peer-reviewed formal professional papers but has less stringent limitations on manuscript length and extent of graphic presentations.
- **TECHNICAL MEMORANDUM.** Scientific and technical findings that are preliminary or of specialized interest, e.g., quick release reports, working papers, and bibliographies that contain minimal annotation. Does not contain extensive analysis.
- **CONTRACTOR REPORT.** Scientific and technical findings by NASA-sponsored contractors and grantees.

- **CONFERENCE PUBLICATION.** Collected papers from scientific and technical conferences, symposia, seminars, or other meetings sponsored or cosponsored by NASA.
- **SPECIAL PUBLICATION.** Scientific, technical, or historical information from NASA programs, projects, and missions, often concerned with subjects having substantial public interest.
- **TECHNICAL TRANSLATION.** English-language translations of foreign scientific and technical material pertinent to NASA's mission.

Specialized services that complement the STI Program Office's diverse offerings include creating custom thesauri, building customized databases, organizing and publishing research results . . . even providing videos.

For more information about the NASA STI Program Office, see the following:

- Access the NASA STI Program Home Page at <http://www.sti.nasa.gov>
- E-mail your question via the Internet to help@sti.nasa.gov
- Fax your question to the NASA Access Help Desk at 301-621-0134
- Telephone the NASA Access Help Desk at 301-621-0390
- Write to:
NASA Access Help Desk
NASA Center for AeroSpace Information
7121 Standard Drive
Hanover, MD 21076



Plasma Emission Characteristics From a High Current Hollow Cathode in an Ion Thruster Discharge Chamber

John E. Foster and Michael J. Patterson
Glenn Research Center, Cleveland, Ohio

Prepared for the
38th Joint Propulsion Conference and Exhibit
cosponsored by the AIAA, ASME, SAE, and ASEE
Indianapolis, Indiana, July 7-10, 2002

National Aeronautics and
Space Administration

Glenn Research Center

Trade names or manufacturers' names are used in this report for identification only. This usage does not constitute an official endorsement, either expressed or implied, by the National Aeronautics and Space Administration.

This report contains preliminary findings, subject to revision as analysis proceeds.

Available from

NASA Center for Aerospace Information
7121 Standard Drive
Hanover, MD 21076

National Technical Information Service
5285 Port Royal Road
Springfield, VA 22100

Available electronically at <http://gltrs.grc.nasa.gov>

Plasma Emission Characteristics From a High Current Hollow Cathode in an Ion Thruster Discharge Chamber

John E. Foster and Michael J. Patterson
National Aeronautics and Space Administration
Glenn Research Center
Cleveland, Ohio 44135

The presence of energetic ions produced by a hollow cathodes operating at high emission currents ($>5A$) has been documented in the literature. In order to further elucidate these findings, an investigation of a high current cathode operating in an ion thruster discharge chamber has been undertaken. Using Langmuir probes, a low energy charged particle analyzer and emission spectroscopy, the behavior of the near-cathode plasma and the emitted ion energy distribution was characterized. The presence of energetic ions was confirmed. It was observed that these ions had energies in excess of the discharge voltage and thus cannot be simply explained by ions falling out of plasma through a potential difference of this order. Additionally, evidence provided by Langmuir probes suggests the existence of a double layer essentially separating the hollow cathode plasma column from the main discharge. The radial potential difference associated with this double layer was measured to be of order the ionization potential.

Nomenclature

Introduction

D_{\perp}	=	Electron cross-field diffusion coefficient
e	=	Elementary charge of an electron
E	=	Ion energy
E_r	=	Sheath electric field
J_e	=	Electron cross-field current density
n_e	=	Electron number density
μ	=	Electron mobility
L	=	Distance between ESA and entrance
n_e	=	Electron number density
R	=	Electrostatic energy analyzer mean radius
r	=	Radial location
r_1	=	Radius of inner sector of electrostatic energy analyzer
r_2	=	Radius of outer sector of electrostatic energy analyzer
V_p	=	Plasma potential measured with respect to cathode potential
U	=	Upper level excited state energy
ΔE	=	ESA energy resolution
ΔV	=	Potential difference between ESA spherical sectors
ϕ	=	Sector angle
ω	=	Entrance aperture diameter

Deep space missions utilizing ion thrusters will require very long thrusting times. Such long operation times place demanding requirements on the lifetime of thruster components. Components such as the ion optics and the discharge and neutralizer hollow cathodes are continuously subjected to erosion processes driven primarily by ion bombardment via either direct impingement or charge exchange. Hollow cathodes are peculiar in that not only are they subjected to ion bombardment from the surrounding discharge plasma, but also, as evidence suggests, they may actually be the source of very energetic ions that can enhance erosion of itself as well as erosion of upstream surfaces such as the screen grid. Indeed it was the erosion of internal discharge chamber structures such as the cathode baffle that led to the first suppositions hinting at the existence of a energetic heavy particle beam emanating from the discharge cathode. Studies led by Manteneiks,¹ Rawlin,² and Brophy/Garner³ all observed severe baffle erosion that was suggestive of energetic ion bombardment. Brophy/Garner³ postulated that the observed severe cathode baffle erosion was due to energetic heavy particle bombardment, presumably energetic xenon ions. Findings from these studies eventually led to the initiation of studies aimed at determining the underlying mechanism for the observed erosion. The bell jar studies of Wilbur⁴ determined that there were indeed very energetic ions originating at the discharge hollow cathode. These studies indicated that the magnitude of the energetic ion component increases with increasing discharge current. To date, the production of energetic ions in hollow cathode

discharges has been documented by a number of studies.^{4,5,6} Theories attempting to describe the production mechanisms of these ions range from the existence of a potential hill,^{4,6,7} to magnetohydrodynamic⁵ effects to hydrodynamic drag driven primarily by electron-ion collisions.⁸ Presently, however, there has been no satisfactory complete explanation offered for the production of the energetic ions.

The purpose of the study presented here is to add to the body of knowledge regarding energetic ion production in high current hollow cathode discharges. The study presented here is unique in that the ion energy distribution is measured in a multi-cusp magnetic environment characteristic of ion thruster operation. In this respect the findings are likely more representative of ion thruster operation in regards to plasma production mechanisms and in particular plasma containment by the axial magnetic field in the near-cathode region.⁹

In addition to the analysis of the ion efflux from the cathode, the near-cathode plasma was probed with Langmuir and emission spectroscopy probes to measure local plasma properties such as density and plasma potential. Langmuir probe measurements were used to survey axial and radial plasma potential profiles. The emission spectroscopy measurements were used to detect the presence of doubly charged xenon ions. These data provides additional insight into the possible physical mechanisms of energetic ion production as well as useful insight into other possible erosion phenomena at the cathode.

Experimental set-up

The experiments were conducted in a 91 cm long by 48 cm in diameter cryopumped bell jar shown in Figure 1. The “bell”, which was made of Pyrex[®], allowed for excellent visual inspection of the discharge. The discharge itself was generated using a 12.7 mm diameter hollow cathode. The cathode assembly included a coaxial keeper electrode. This electrode was not biased during this investigation. The hollow cathode was installed in a three-magnet ring, 30-cm discharge chamber of similar geometry to that of the NASA Solar Electric Propulsion Technology Application Readiness (NSTAR) thruster. Again, the choice of conducting the investigation of energetic ion efflux using a hollow cathode in a ring cusp discharge chamber was made primarily to determine the nature of the ion efflux in a thruster-like environment. The magnetic field near the cathode tip was approximately 90 G. For this study the hollow cathode was operated grounded.

The energy distribution of the ion flux emanating from the hollow cathode was characterized using an electrostatic spherical sector energy analyzer (ESA).

The ESA was located on axis with the hollow cathode, separated by approximately 23 cm. A schematic of this experimental set-up is illustrated in Figure 2. The analyzer consisted of two spherical sectors (141 degrees in this case) in which the potential of each relative to ground was varied. The potentials on these surfaces determine the energy of which an entering particle must have in order to pass through from entrance slit to exit slit. In this respect, the ESA can be operated as an energy selector. The energy of the particles that can pass through can be calculated based on the geometry and potential difference between the spherical surfaces:

$$E = \frac{\Delta V}{\frac{r_1}{r_2} - \frac{r_2}{r_1}} \quad (1)$$

with an energy resolution also determined by geometry and energy:

$$\frac{\Delta E}{E} \approx \frac{\omega}{R \cdot (1 - \cos \phi) + L \cdot \sin \phi} \quad (2)$$

The ESA was operated in a constant transmission energy mode. A schematic of the electrical connections for operation and data acquisition from the ESA is illustrated in Figure 2b. The transmission energy as determined by the potential difference between the two spherical surfaces was set at 10 eV. With this transmission energy, the energy resolution was approximately 0.347 eV. The input slit varied in potential so that ions with energies between 0 and approximately 100 eV could be scanned. This factory recommended mode of operation is similar to that used by Kameyama and Wilbur in their investigation of ion efflux from high current hollow cathodes.⁶ The ESA was housed in an iron box so as to reduce the effect of the local magnetic field generated by the thruster discharge chamber. The magnetic field at the entrance slit of the ESA was less than 1 G. In order to minimize the flow of plasma into the device, a cup made of very fine, electro-etched nickel was placed over the entrance slit. The mesh make-up was 20 lines per mm with a 0.039 mm spacing between lines. The nickel wire that made up the mesh was 0.01 mm in diameter. The mesh and the iron box were fixed at ground potential. The electrostatic energy analyzer was suspended over the discharge chamber via a perforated aluminum termination plate. The plate, which located roughly 8.5 cm downstream of the discharge exit plane, contained 8–5.5 cm diameter holes and one 8.5 cm in diameter center hole. This plate was operated at cathode potential during this investigation. This open geometry was chosen because of its higher conductivity of neutrals away from the discharge chamber as

compared to discharge studies with a simulated grid terminating the exit plane. The open geometry of the test apparatus allows the discharge pressure to be maintained at values similar to that of the bell jar. Because the bell jar pressures are similar to those that prevail in ion thrusters (~ 0.013 Pa ($\sim 1 \cdot 10^{-4}$ Torr)), the discharge characteristics are expected to be similar to actual ion thruster operation, thereby circumventing issues associated with gridded discharge studies.¹⁰ This notion is supported by the modest discharge voltages measured (many of which were similar in magnitude to NSTAR engine operation (~ 26 V)).

The near-cathode plasma in the discharge chamber was characterized using three Langmuir probes located axially in the near vicinity of the plane that contains the keeper face (see Figure 2). The near-cathode probes tips were made from tungsten wire and were 0.38 mm in diameter and 3 mm long. Two of the probes also contained optical fibers to record line-integrated emission in this plane. This was accomplished using double bore alumina tubing. One bore contained the Langmuir probe tip while the other contained a recessed optical fiber. The fibers were recessed approximately 1 cm upstream of the bore opening to aid in the collimation of the collected light. The optical fiber had a core size of 400 micrometers and an aluminum protective outer sheath. These probes were positioned at a variety of locations ranging from near the anode wall to nearly on discharge axis in order to determine the potential and density distribution in the plane of the keeper. A fourth probe, 5.5 mm long, 0.38 mm in diameter was used to measure plasma properties near the entrance slit of the ESA.

The plasma induced emission collected by the optical fibers was channeled to a 0.25 m spectrometer fitted with a photo-multiplier tube. The spectrometer contained a 1200 lines/mm grating blazed at 350 nm.

Experimental Results and Discussion

Ion Energy Distribution Measurements

The ion energy distribution was measured as a function of discharge current at a fixed flow rate of 4 standard cubic centimeters per minute (SCCM). For all operating conditions, the bell jar pressure never exceeded 1.5×10^{-4} Torr. The discharge conditions investigated varied from 10 A to 22 A corresponding to discharge voltages varying between 26 V and 29 V. Before plasma measurements were taken, the discharge was allowed to stabilize at each operating condition. In all cases, the peak-to-peak oscillations in the discharge voltage were less than 3 volts.

Figure 3a shows typical variations in voltage as a function of discharge current. As can be seen here,

initially the discharge voltage increases linearly with increasing discharge current up to nearly 16 A, at which point the discharge voltage appears to saturate. Figure 3b shows the variations in the ion energy distribution function at the different discharge currents. As can be seen here, the collected current at energies less than 8 eV did not have a strong dependence on energy. The slowly varying ion current collected in this range is likely due to low energy charge exchange ions generated between the nickel mesh and input aperture of the ESA. Such low energy ions have been observed in ESA spectra under similar conditions elsewhere.⁶ The location of the primary peak of the ion current distribution did not vary appreciably with increasing discharge current. Its average value was approximately 14 eV. The ions associated with this peak are due to ions accelerated into the detector due to the potential difference between the discharge plasma and the detector. In this case, the data suggests that the fall voltage between the detector and the plasma (on axis) was of order 14 V. This value should be representative of the potential difference between the discharge plasma and cathode potential surfaces. Interestingly, the potential difference between the plasma and the detector was not the discharge voltage. Consistent with this observation, Langmuir probes located near (~ 2 cm off axis) the ESA entrance slit indicated plasma potentials ~ 10 V less than the discharge voltage. These data suggest that the potential difference between the screen and discharge plasma in an actual ion thruster may also be less than the discharge voltage. In this case, ions do not enter screen grid apertures at the discharge voltage, but instead at a reduced energy.

It is interesting to note that the primary peak of the ion energy distribution was in all cases Gaussian in shape. The width of the peak tended to increase with increasing discharge current, from 14 eV at 10.5 A to over 21 eV at 18.3 A. Apparently the energy spread increases with increasing discharge current. Also according to Figure 3b, as the discharge current increases, the overall magnitude of the collected ion current at a given energy increases. Additionally, as with the increase in width of the primary peak, the extension of the edge of the distribution into higher energies increases with increasing discharge current. This implies that with increasing discharge current, the population of energetic ions increase. In this respect the ion current distribution may be characterized best as a Gaussian with a superthermal tail that increases in magnitude with increasing discharge current. The primarily Gaussian nature of the ion current distribution differs significantly from that observed in similar hollow cathode studies conducted in the absence of an ion thruster discharge chamber.^{4,6} In those cases, the distribution consisted of multiple peaks, some of which

were centered at energies well above the discharge voltage. It is likely that the presence of the magnetic field in the ion thruster discharge chamber of this present study, particularly the axial component, plays a key role in accounting for the differences.

In order to assess the changes in the energetic component of the ion current distribution, the ratio of energetic ion current associated with energies 27 eV and above to the total ion current collected over the energy range investigated was calculated. The value, 27 eV, was chosen because it represents the lower limit for threshold sputtering of molybdenum by xenon ions.¹² Molybdenum is a metal typically used in the construction of the cathode keeper and screen and accelerator grid electrodes. Because the low energy, charge exchange ion (see Figure 3b) flux incident upon the ESA slit are an artifact of the experimental set-up and are therefore not representative of actual ion flux emanating from outside the protective mesh, their contribution to the total ion current collected over the energy range investigated is neglected. The energy range containing the low energy ions was determined by taking the derivative of the distribution function to locate the region of the curve where the low energy ions contribution ended. It was assumed that the relevant ion distribution began at the knee of the derivative as illustrated in Figure 4a. Figure 4b shows the variations of ion current distribution function at energies just beyond the knee.

Figure 5 illustrates the behavior of the energetic ion current fraction ($E > 27\text{eV}$) as a function of discharge current. As can be seen here the fraction of energetic ions on axis with energies capable of eroding cathode potential surfaces such as the screen grid tends to increase monotonically with discharge current. This finding is also similar to that observed by Kameyama and Wilbur.⁶ Also shown on the plot is a trendline which indicates a nearly quadratic increase in the energetic ion fraction with increasing discharge current. As can be seen in the plot, at discharge currents over 18 A, nearly 15% of the ion current on axis have energies capable of eroding discharge chamber surfaces such as the screen grid. It should be pointed out that the ESA does not distinguish between different ion charge states. The energetic ion current detected is likely comprised of some fraction of doubly charged ions. This is to be expected because the discharge voltage under the operating conditions investigated was sufficiently high to generate doubly charged xenon. With this in mind, the energetic ion current fraction as determined here could be used to determine an upper bound on the axial energetic ion particle flux used in simple erosion calculations.

Near-Cathode Plasma Properties

Discharge plasma conditions were documented in the near-cathode region using Langmuir probes and emission spectroscopy. The Langmuir probes were used to measure the plasma density and potential distribution radially in the plane of the keeper and axially just downstream of the keeper. The emission spectroscopy was used primarily for the detection of the various xenon charge states in the discharge.

B-field effects

The axial magnetic field profile associated with the ring cusp magnetic circuit influences the nature and coupling of the hollow cathode discharge to the main discharge plasma. It is expected that the magnetic environment should significantly influence discharge plasma properties particularly in the near-cathode region. The axial field near the cathode tends to confine the hollow cathode external positive column. This field can significantly reduce radial electron diffusion and therefore plays a role in determining discharge impedance and stability. Axial plasma electrical conductivity is enhanced by the presence of the axial magnetic field. Electrons resulting from ionization along the axis cannot readily diffuse radially because of the constraining effects of the magnetic field. This effect coupled with the enhanced axial electrical conductivity would tend to smooth out potential structures on axis particularly in the region close to the cathode where the axial field is large (~90 G). This reasoning is supported by Langmuir probe measurements made near the axis at 3 mm and 9 mm downstream of the keeper. It was found that the plasma potential at these probes was within experimental error virtually the same. In this regard, potential hill phenomena may not be as important in the production of energetic ions in actual ion thrusters due to the smoothing effects of the axial magnetic field.

Finally, as mentioned earlier, electron “friction” was described as a possible mechanism for the formation of energetic ions. This theory postulates that energetic ions are formed due to a high rate of electron-ion collisions.⁸ According to the theory, if the electron-ion collision frequency is sufficiently high, then ions can absorb significant amounts of energy, well in excess of the discharge voltage. This effect should depend on axial magnetic field particularly in the near cathode region. The containment of the hollow cathode plasma by the axial magnetic field would tend to increase the electron-ion collision frequency.

Potential distributions

Qualitatively, visual observation of the discharge chamber operating suggests that the discharge plasma actually consists of two components: a hollow cathode plasma contained primarily by the axial magnetic field and a main discharge. Figure 6 qualitatively illustrates this notion. The hollow cathode external positive column appears as a conical plume fanning out from the orifice of the discharge cathode. The discharge glow is brightest here. Again, this conically shaped discharge emanating from the hollow cathode is a consequence of the axial magnetic field confining the external positive column of the hollow cathode. With increasing axial distance the axial magnetic field decreases and therefore the fanning effect (weaker containment) is observed.

As mentioned earlier, local to the near-cathode region, no appreciable axial potential gradient was detected. Interestingly, however, it was found that a significant radial potential gradient existed in the plane of the keeper. This potential gradient (and associated electric field, E_r) is apparently associated with the transition from the hollow cathode positive column to the main discharge plasma and is required to aid the diffusion of electrons across the axial magnetic field to the anode:

$$J_e = -e \cdot \mu \cdot n_e \cdot E_r - e \cdot D_{\perp} \cdot \frac{dn_e}{dr} \quad (3)$$

It is also interesting to note that this potential gradient was of order the ionization potential of xenon. In this regard, the gradient imparts radial energies to electrons formed in the hollow cathode external positive column so that ionization can take place as the electrons move radially toward the anode. This free-standing gradient structure indicates the presence of a double layer.¹³ Double layers are free-standing potential structures that form the transition between two plasmas (in this case the cathode and the bulk discharge) that are at two different potentials. In this case the cathode column is at a lower potential than the main discharge. Figure 7a illustrates the variations in the plasma potential at various radial positions in the plane of the cathode keeper. As can be seen in the figure, there is a voltage rise of order the ionization potential of Xenon between points near the cathode centerline and the region of plasma just off axis (~1 cm). Beyond this rise, the plasma potential off axis, however, does not vary appreciably with increasing radial distance. As illustrated in Figure 7b, the plasma density profile also follows the trends similar to the potential. Plasmas density drops very sharply across the presumed double layer. In this respect, the hollow cathode plasma

represents the high-density core of a composite discharge.

The voltage gradients are expected to be highest at the cathode orifice because the axial magnetic field (radial impedance) is strongest there. The effect of the double layer potential structure would be to accelerate ions that happen to enter this region toward keeper and cathode structures, possibly giving rise to a radially directed erosion component. It is possible that the double layer structure may have played a role in the anomalous keeper erosion recorded during the NSTAR ion thruster long duration life test conducted at the NASA Jet Propulsion Laboratory.¹⁴ If the cathode was operating in a starved condition, then it can be expected that the double layer voltage drop would be quite large, perhaps of order the discharge voltage. A double layer potential difference of this magnitude would accelerate electrons to energies necessary to create singly and doubly charged ions directly. The double layer potential difference would accelerate these ions into the cathode and keeper electrodes.

Emission Spectroscopy

Emission spectra were obtained from fibers that collected collimated light along the radius of the discharge chamber in the plane of the cathode keeper. In all cases the most intense lines were the Xe II transitions. Figure 9 illustrates the behavior of the 484 nm Xe II line and the 467 Xe I line as a function of discharge current. In general, all emission lines tended to increase in intensity with increasing discharge current. This behavior is likely associated with the corresponding increase in plasma density and thus associated excitation rates. One primary function of the emission spectroscopy diagnostic was to investigate the presence of doubly charged ions. At all discharge currents investigated, no Xe III lines were found in the spectra. This finding suggests that the absence in signal associated with these lines may be due to the absence of electrons with the energy necessary to excite them. It should be pointed out that Xe III lines with low excitation energies (~12 eV) can be found in the vacuum ultraviolet. These lines should be present. Such measurements, however, were beyond to capability of the spectroscopy system used in this investigation and therefore were not made. Instead, the spectra was analyzed for the presence of xenon singly charged lines with comparable excitation energies as Xe III ions in the visible range. In the visible, the excitation energy for the Xe III 472.3 nm line is 18.2 eV. The Xe II 431 (U=18.14 eV) and Xe II (U=17.9 eV) have comparable excitation energies as the Xe III 472.3 nm line.¹⁵ These singly charged ion lines were observed in the spectra, suggesting that electrons with energy

comparable to that required to excite the Xe III lines in the visible were indeed present. The spectra of these energetic lines are illustrated in Figure 10. It was observed that these lines increased in intensity monotonically with increasing discharge current suggesting that the energetic electron population also grew with increasing discharge current. These findings suggest that the doubly charged xenon population is likely present, but their emission is below the sensitivity of the spectrometer system used.

Conclusion

The energy distribution of ions flowing axially downstream from a hollow cathode was investigated using a NSTAR-type ring cusp discharge chamber. It was found that the energy distribution extended to higher energies as the discharge current increased. At the higher discharge currents, the fraction of ions on axis with energies above the sputtering threshold for molybdenum, a typical ion optics material, was nearly 15% at the higher discharge currents investigated. Near-cathode plasma potential measurements revealed the presence of a double layer separating the hollow cathode plasma from the main discharge plasma. This potential difference contributes to electron diffusion across field lines to the anode. This same potential difference, however, could drive ion bombardment erosion of cathode and keeper surfaces. Doubly charged xenon ion lines were not observed in the spectra. The absence of such emission lines in the measured spectra may be due to insufficient optical sensitivity.

References

¹Manteniaks, M.A. and Rawlin, V.K., "Studies of Internal Sputtering in a 30-cm Ion Thruster," 11th Electric Propulsion Conference, New Orleans, Louisiana, March 19–21, 1975.
²Rawlin, V.K., "Internal Erosion Rates of a 10-kW Xenon Ion Thruster," AIAA Paper 88–2913, 24th Joint Propulsion Conference, Boston, Massachusetts, July 11–13, 1988.

³Brophy, J.R. and Garner, C.E., "Tests of High Current Hollow Cathodes for Ion Engines," AIAA Paper 88–2913, 24th Joint Propulsion Conference, Boston, Massachusetts, July 11–13, 1988.

⁴Friedly, V.J. and Wilbur, P.J., "High Current Hollow Cathode Phenomena," *Journal of Propulsion and Power*, Vol. 8, No. 3, May–June, 1992, pp. 635–643.

⁵Latham, P.M., Pearce, A.J., and Bond, R.A., "Erosion Processes in the UK-25 Ion Thruster," IEPC Paper 91–096, 22nd International Electric Propulsion Conference, Viareggio, Italy, October 14–17, 1991.

⁶Kameyama, Ikuya and Wilbur, P.J., "Measurements of Ions from High Current Hollow Cathodes Using Electrostatic Energy Analyzer," *Journal of Propulsion and Power*, Vol. 16, No. 3, May–June 2000, pp. 529–535.

⁷Davis, W.D., and Miller, H.C., "Analysis of the products emitted by dc arcs in a vacuum ambient," *J. Appl. Phys.*, Vol. 40, pp. 2212–2221, 1969.

⁸Hantzsche, E., "A Hydrodynamic Model of Vacuum Arc Plasma," *IEEE Transactions on Plasma Science*, Vol. 20, No. 1, February 1992.

⁹Delcroix, J. and Trindade, A.R., "Hollow Cathode Arcs" in *Advances in Electronics and Electron Physics*, Marton, L. ed., Vol. 35, Academic Press, NY, pp. 109–145, 1974.

¹⁰Brophy, J.R., "Simulated Ion Thruster Operation without Beam Extraction," AIAA, DGLR, and JSASS 21st International Electric Propulsion Conference, Orlando, FL, 1990, AIAA Paper 90–2655.

¹²Stuart, R.V. and Wehner, G.K., "Sputtering yields at very low bombarding energies," *Journal of Applied Physics*, vol. 33, no. 7, July 1962, pp. 2345–2352.

¹³Coakley, P. and Hershkowitz, N., "Laboratory double layers," *Phys. Fluids*, vol. 22, no. 6, June, 1979, pp. 1171–1181.

¹⁴Polk, J.E. et al., "An overview of results from the 8200 hr Wear test of NSTAR ion thruster," AIAA Paper No. 99–2446, Los Angeles, 1999.

¹⁵Striganov, A.R. and Sventitskii, N.S., *Tables of Spectral Lines of Neutral and Ionized Atoms*, IPI Plenum, New York, 1968, pp. 571–607.

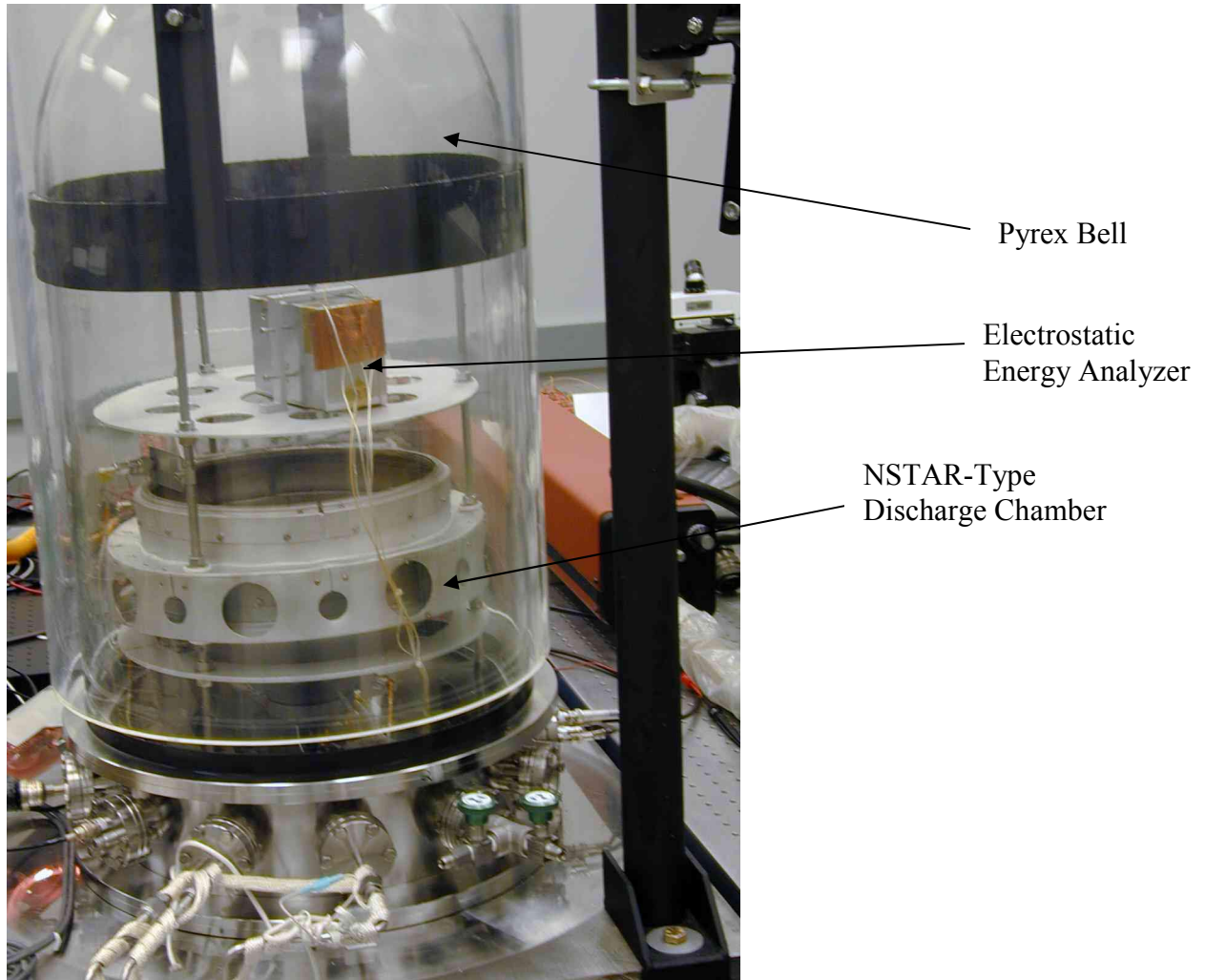


Figure 1. Bell jar used in this investigation. Note position of discharge chamber and electrostatic energy analyzer.

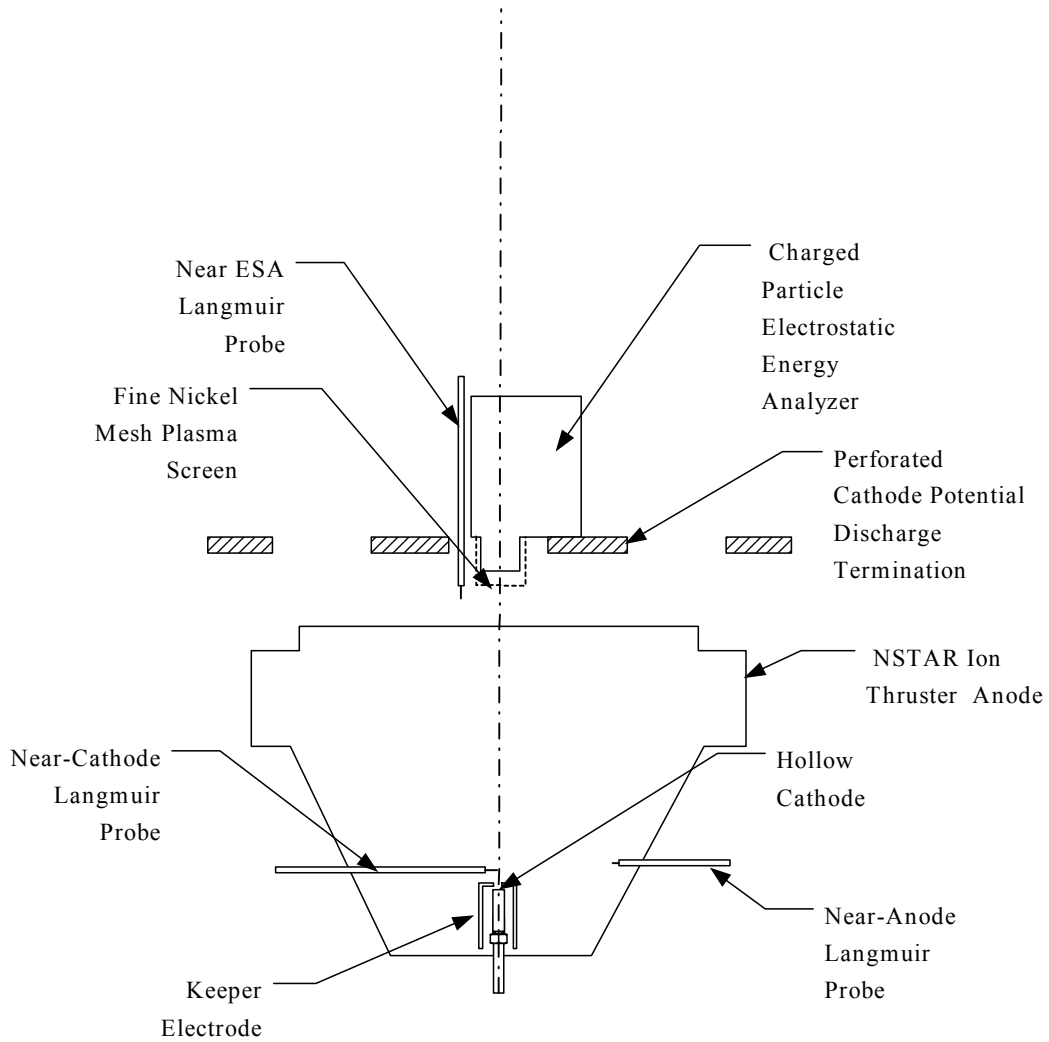


Figure 2a. Schematic of experimental set-up. Note location of the Langmuir probes and the ESA.

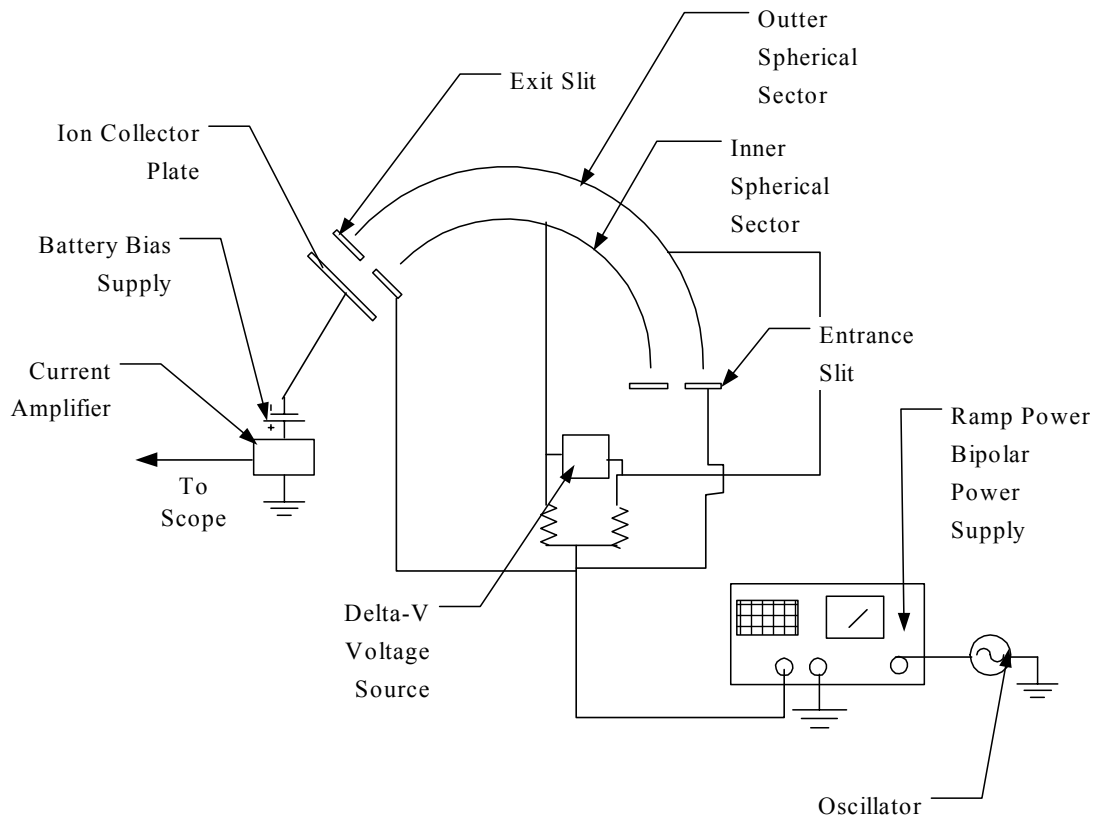


Figure 2b. Pictorial representation of the electrical connections to ESA for constant transmission energy mode.

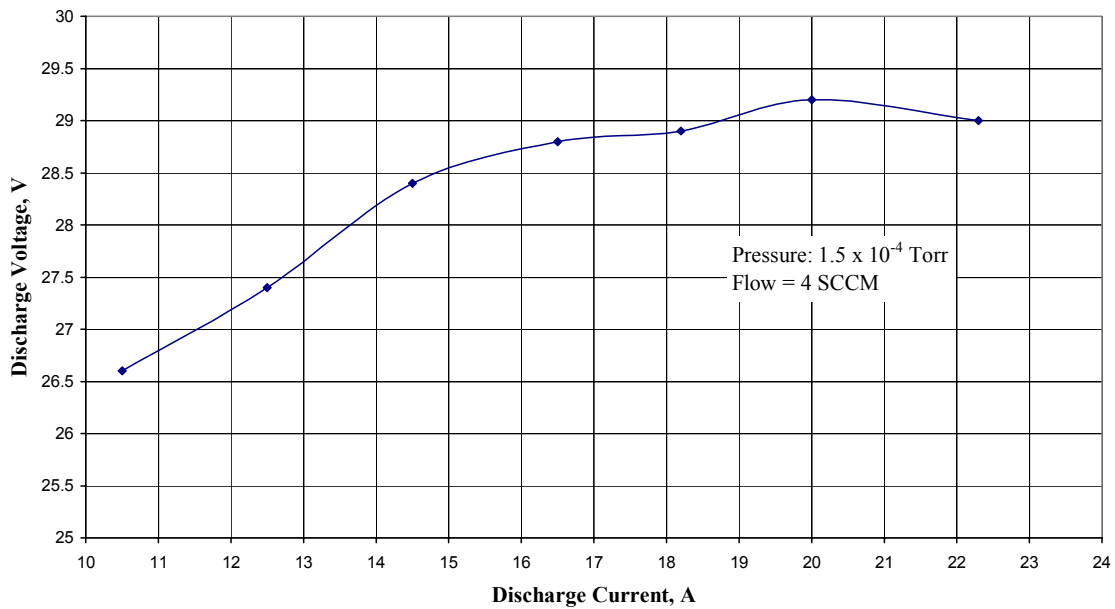


Figure 3a. Discharge characteristics of NSTAR discharge chamber at fixed flow rate.

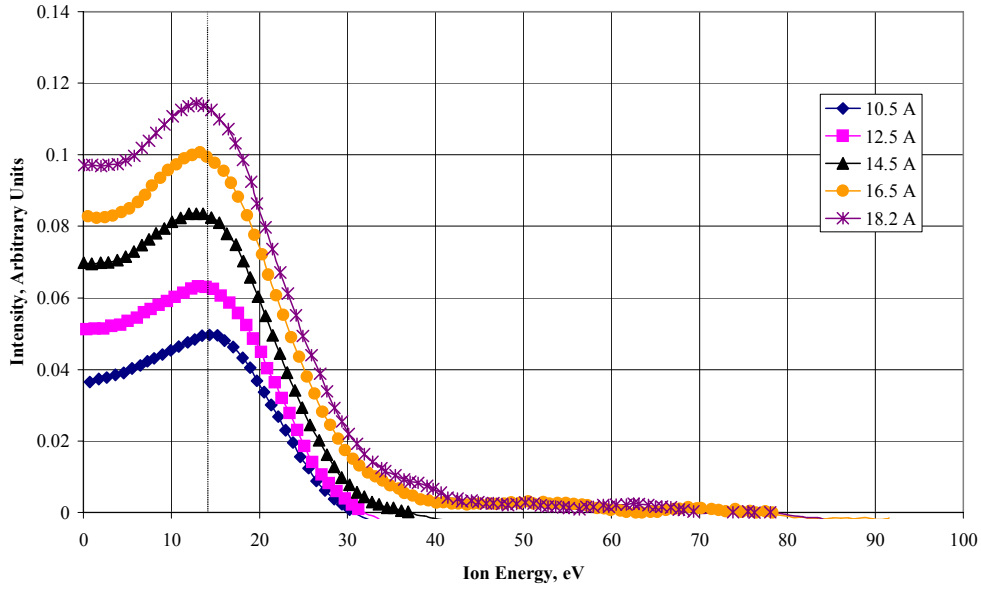


Figure 3b. Variations in the ion energy distribution with increasing discharge current.

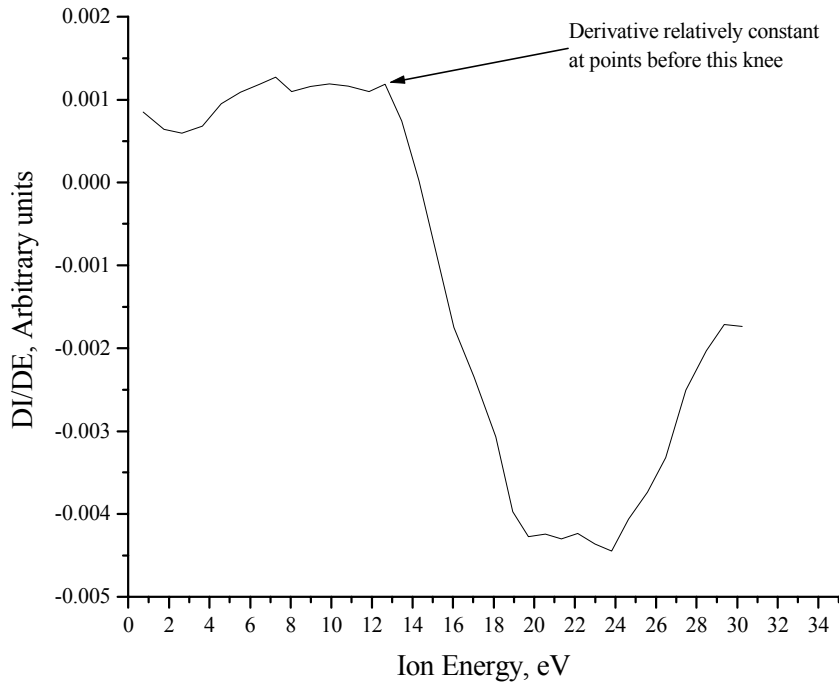


Figure 4a. Derivative of the ion current signal as a function of ion energy. The slowly varying region at low energies is due to background charge-exchange ions. Discharge current=10.5 A.

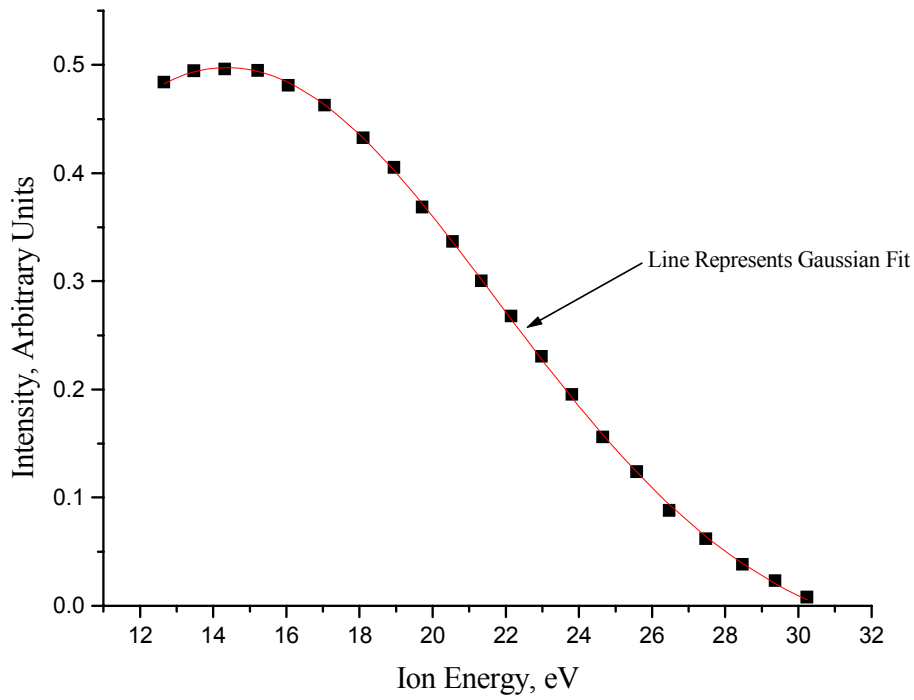


Figure 4b. Gaussian fit to 10.5 A case with low energy ion contribution removed.

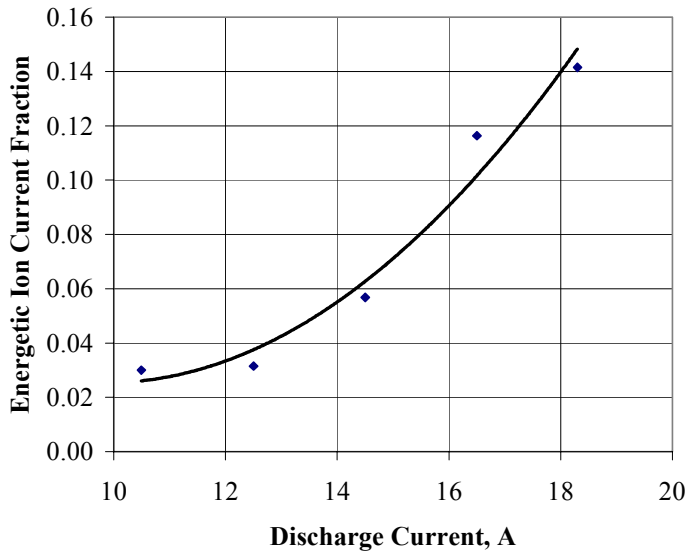


Figure 5. Variation in the energetic ion current fraction (ions with kinetic energies above 27 eV) with increasing discharge current.

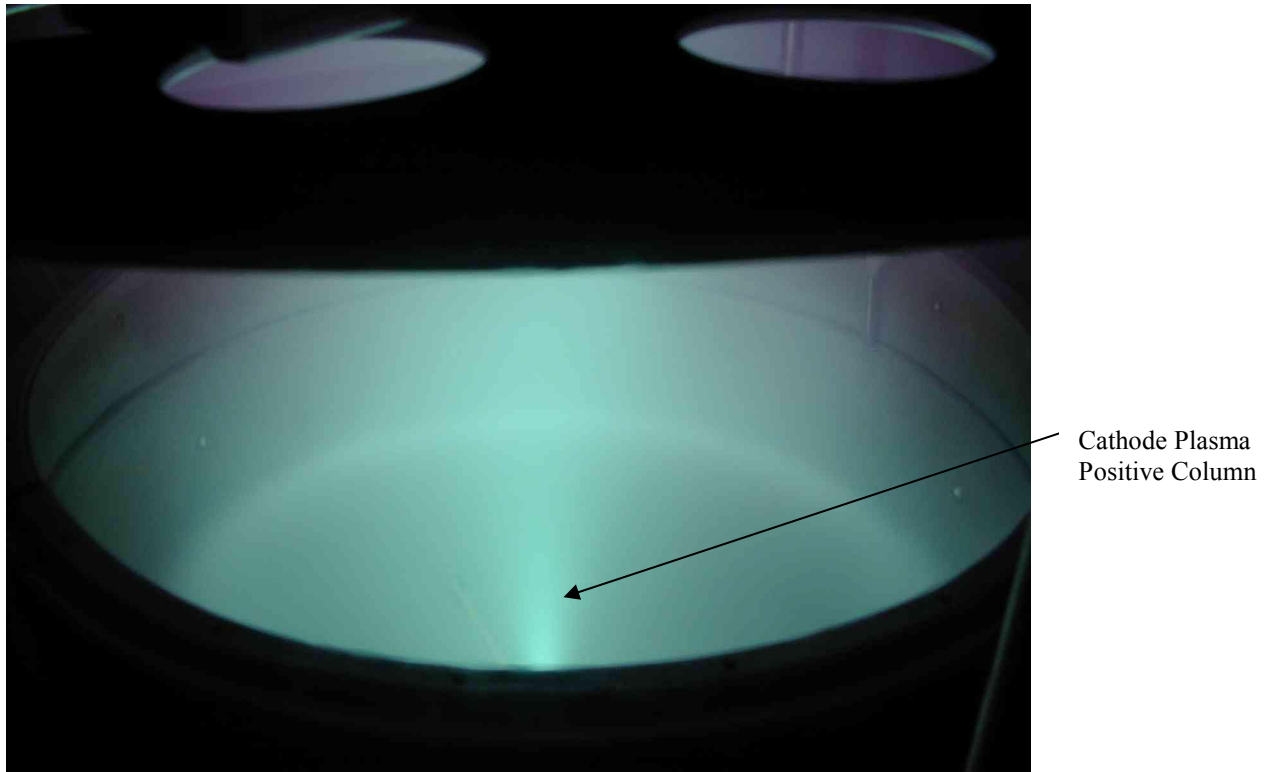


Figure 6. Discharge operation: Notice cathode plasma (plume emanating from discharge cathode) and main discharge plasma, which appears more diffuse and weaker in intensity.

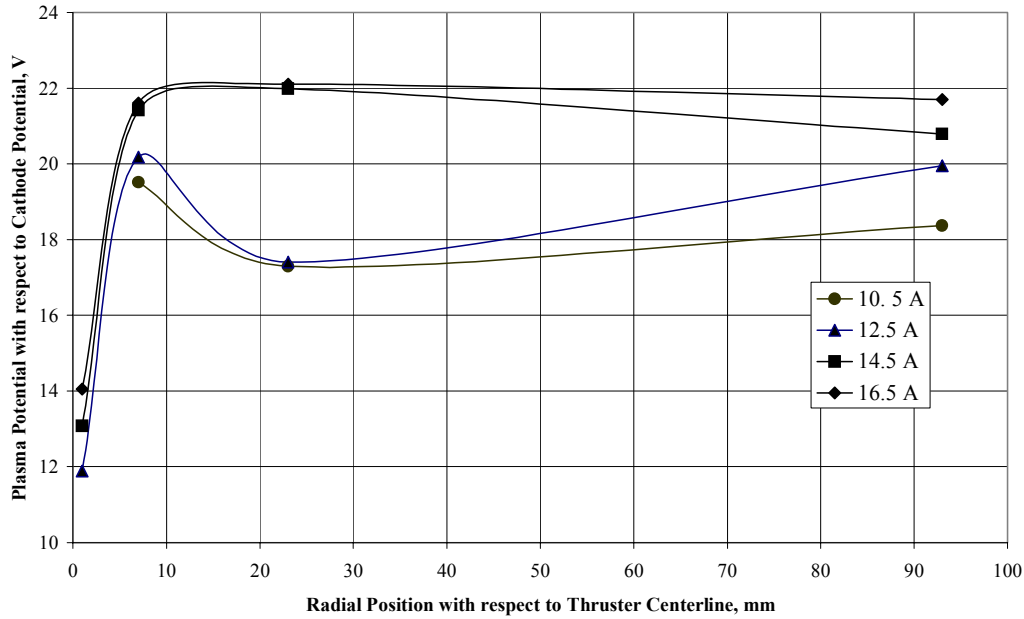


Figure 7a. Radial plasma potential variations at different discharge currents. Profiles are indicative of a double layer. Probe located 3 mm downstream of keeper plane.

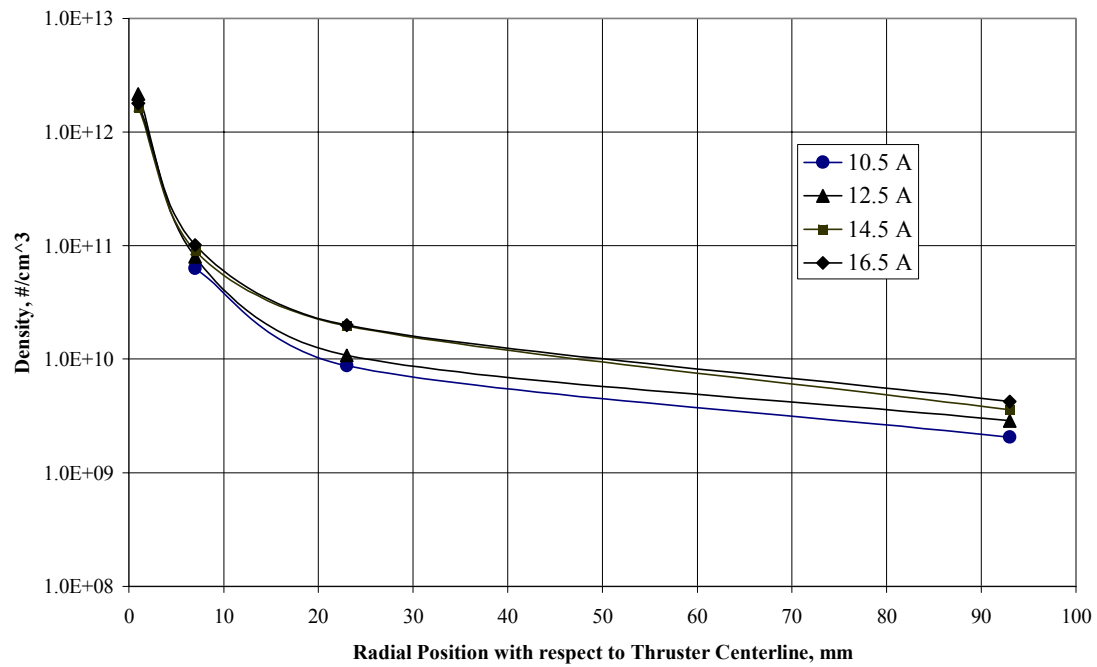


Figure 7b. Radial plasma density variations as a function of discharge current. Probe located 3 mm downstream of keeper plane.

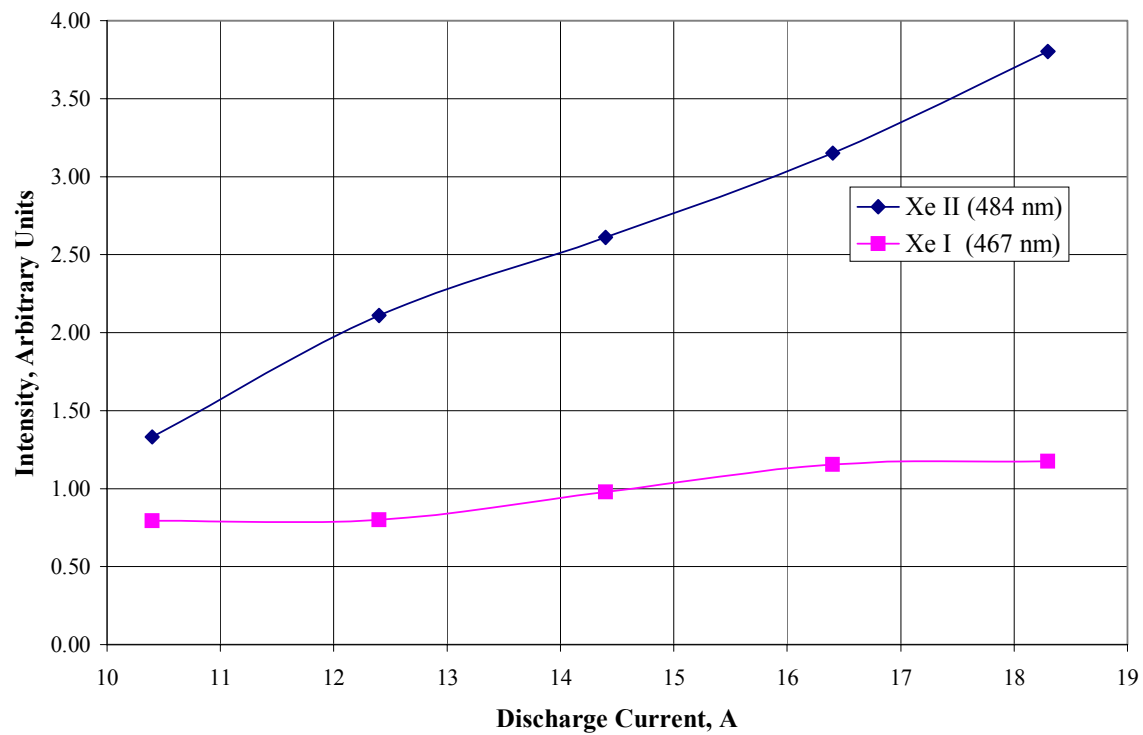


Figure 8. Variation in ion and neutral emission with increasing discharge current.

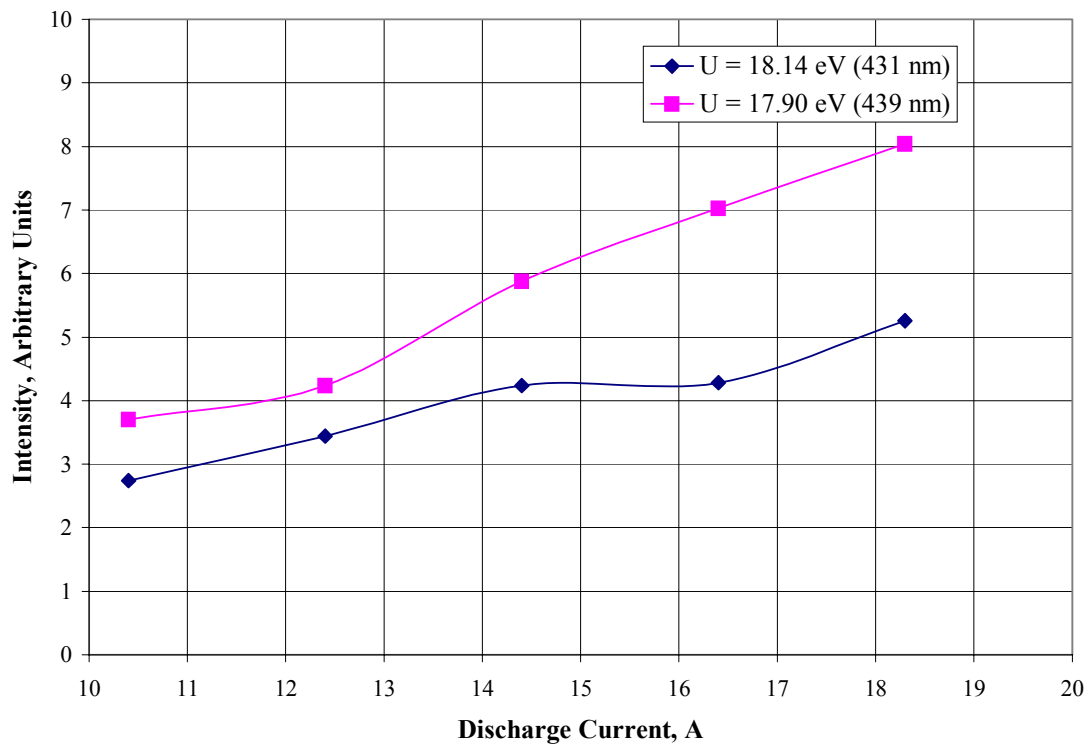


Figure 9. Variations in xenon ion lines requiring energetic electrons (~18 eV) for excitation of transition with discharge current.

REPORT DOCUMENTATION PAGEForm Approved
OMB No. 0704-0188

Public reporting burden for this collection of information is estimated to average 1 hour per response, including the time for reviewing instructions, searching existing data sources, gathering and maintaining the data needed, and completing and reviewing the collection of information. Send comments regarding this burden estimate or any other aspect of this collection of information, including suggestions for reducing this burden, to Washington Headquarters Services, Directorate for Information Operations and Reports, 1215 Jefferson Davis Highway, Suite 1204, Arlington, VA 22202-4302, and to the Office of Management and Budget, Paperwork Reduction Project (0704-0188), Washington, DC 20503.

1. AGENCY USE ONLY (Leave blank)		2. REPORT DATE November 2002	3. REPORT TYPE AND DATES COVERED Technical Memorandum	
4. TITLE AND SUBTITLE Plasma Emission Characteristics from a High Current Hollow Cathode in an Ion Thruster Discharge Chamber			5. FUNDING NUMBERS WU-755-B4-04-00	
6. AUTHOR(S) John E. Foster and Michael J. Patterson				
7. PERFORMING ORGANIZATION NAME(S) AND ADDRESS(ES) National Aeronautics and Space Administration John H. Glenn Research Center at Lewis Field Cleveland, Ohio 44135-3191			8. PERFORMING ORGANIZATION REPORT NUMBER E-13558	
9. SPONSORING/MONITORING AGENCY NAME(S) AND ADDRESS(ES) National Aeronautics and Space Administration Washington, DC 20546-0001			10. SPONSORING/MONITORING AGENCY REPORT NUMBER NASA TM-2002-211876 AIAA-2002-4102	
11. SUPPLEMENTARY NOTES Prepared for the 38th Joint Propulsion Conference and Exhibit cosponsored by the AIAA, ASME, SAE, and ASEE, Indianapolis, Indiana, July 7-10, 2002. Responsible person, John E. Foster, organization code 5430, 216-433-6131.				
12a. DISTRIBUTION/AVAILABILITY STATEMENT Unclassified - Unlimited Subject Categories: 20 and 75 Available electronically at http://gltrs.grc.nasa.gov This publication is available from the NASA Center for AeroSpace Information, 301-621-0390.			12b. DISTRIBUTION CODE	
13. ABSTRACT (Maximum 200 words) The presence of energetic ions produced by a hollow cathodes operating at high emission currents (>5A) has been documented in the literature. In order to further elucidate these findings, an investigation of a high current cathode operating in an ion thruster discharge chamber has been undertaken. Using Langmuir probes, a low energy charged particle analyzer and emission spectroscopy, the behavior of the near-cathode plasma and the emitted ion energy distribution was characterized. The presence of energetic ions was confirmed. It was observed that these ions had energies in excess of the discharge voltage and thus cannot be simply explained by ions falling out of plasma through a potential difference of this order. Additionally, evidence provided by Langmuir probes suggests the existence of a double layer essentially separating the hollow cathode plasma column from the main discharge. The radial potential difference associated with this double layer was measured to be of order the ionization potential.				
14. SUBJECT TERMS Hollow cathode; Ions; Double layer; Plasma; Electric propulsion; Ion thruster			15. NUMBER OF PAGES 20	
			16. PRICE CODE	
17. SECURITY CLASSIFICATION OF REPORT Unclassified	18. SECURITY CLASSIFICATION OF THIS PAGE Unclassified	19. SECURITY CLASSIFICATION OF ABSTRACT Unclassified	20. LIMITATION OF ABSTRACT	